European Journal of Medicinal Chemistry 44 (2009) 3496–3503

Contents lists available at ScienceDirect

European Journal of Medicinal Chemistry

journal homepage: http://www.elsevier.com/locate/ejmech

Original article

An in vitro characterization study of new near infrared dyes for molecular imaging

Jutta Pauli [a,1], Tibor Vag [b,*,1], Romy Haag [b], Monika Spieles [a], Matthias Wenzel [c], Werner A. Kaiser [b], Ute Resch-Genger [a,**], Ingrid Hilger [b,*]

[a] BAM Bundesanstalt für Materialforschung und –prüfung, OE I.5, Richard-Willstaetter-Str. 11, D-12489 Berlin, Germany
[b] Institut für Diagnostische und Interventionelle Radiologie des Klinikums der Friedrich-Schiller-Universität Jena (IDIR), Forschungszentrum Lobeda, Erlanger Allee 101, D-07747 Jena, Germany
[c] DYOMICS GmbH, Otto-Schott-Str. 15, D-07745 Jena, Germany

ARTICLE INFO

Article history:
Received 3 July 2008
Received in revised form
6 December 2008
Accepted 16 January 2009
Available online 29 January 2009

Keywords:
In vivo fluorescence imaging
NIR fluorophore
Cytotoxicity
Stability
Fluorescence quantum yield
Cyanine

ABSTRACT

The spectroscopic properties, stability, and cytotoxicity of series of cyanine labels, the dyes DY-681, DY-731, DY-751, and DY-776, were studied to identify new tools for in vivo fluorescence imaging and to find substitutes for DY-676 recently used by us as fluorescent label in a target-specific probe directed against carcinoembryonic antigen (CEA). This probe enables the selective monitoring of CEA-expressing tumor cells in mice, yet displays only a low fluorescence quantum yield and thus, a non-optimum sensitivity. All the DY dyes revealed enhanced fluorescence quantum yields, a superior stability, and a lower cytotoxicity in comparison to clinically approved indocyanine green (ICG). With DY-681 and far-red excitable DY-731 and DY-751, we identified three dyes with improved properties compared to DY-676 and ICG.

1. Introduction

Optical imaging techniques, that use light to visualize the optical characteristics of tissue via measurement of its absorption, scattering or fluorescence, have matured into important tools in biomedical research due to advances in instrumentation and label and probe technologies [1–5]. Some applications have meanwhile become part of clinical routine [3,6–9]. Lately, significant attention has been dedicated to fluorescence imaging with near-infrared (NIR) light [10]. This comparatively inexpensive and sensitive spectroscopic technique is capable of noninvasively assessing molecular function in vivo and is thus suited for the detection of very early stages of diseases such as cancer and the monitoring of drug treatment [3,11–15].

Prerequisites for NIR fluorescence (NIRF) imaging are fluorescent labels that can be covalently attached to target-specific ligands like antibodies or antibody fragments for the design of highly specific and sensitive modular fluorescent probes [1–4,10]. Suitable fluorophores must absorb and emit light in the so-called diagnostic window between 650 and 900 nm, where hemoglobin and water absorption is minimum [3], thereby providing the basis for deep tissue penetration of up to several centimeters [2,10]. To realize the desired high sensitivity in localizing tumors or other targets, these fluorophores should reveal a high molar absorption coefficient at the excitation wavelength and a high fluorescence quantum yield [3,16,17]. Also, the concentration of the fluorophore at or in the target should be high and the fluorescence background in the tissue should be at a minimum. This renders especially near-infrared-excitable chromophores intensively absorbing and emitting between 700 and 900 nm attractive [18–20]. Other prerequisites are minimum nonspecific binding, sufficient thermal and photochemical stability, and low cytotoxicity.

Despite of the recognized potential of NIRF imaging and the corresponding importance of rationally designed and well characterized fluorescent labels and probes, until now, the only clinically approved NIR fluorescent dye is indocyanine green (ICG). This

* Corresponding authors. Tel.: +49 (0) 3641 9325921; fax: +49 (0) 3641 9325922.
** Corresponding author. Tel.: +49 (0) 30 8104 1134; fax: +49 (0) 30 8104 1157.
E-mail addresses: tibor.vag@med.uni-jena.de (T. Vag), ute.resch@bam.de (U. Resch-Genger), ingrid.hilger@med.uni-jena.de (I. Hilger).
[1] Both authors contributed equally to this work.

0223-5234/$ – see front matter © 2009 Elsevier Masson SAS. All rights reserved.
doi:10.1016/j.ejmech.2009.01.019

NIR emitting carbocyanine dye [21], that absorbs and emits between approximately. 730 and 900 nm, is used e.g. for angiography of the choroid and for the evaluation of hepatic and cardiac circulation. However, ICG suffers from many drawbacks like a very low fluorescence quantum yield of 0.01 in aqueous solution [22], binding to plasma proteins [23,24], resulting in rapid elimination through the liver, and a low stability in aqueous media [23–26]. Moreover, despite its approval, it reveals a certain cytotoxicity as has been only recently demonstrated [27–29].

The search for new diagnostic tools recently encouraged us to use DY-676, a substitute for Cy5 tailored to match the line of the 680-nm diode laser of the whole body NIRF imaging set up, for the design of a new target-specific probe directed against carcinoembryonic antigen (CEA), a glycoprotein expressed on the cell surface of certain cancer types [30]. This probe revealed an excellent specificity for CEA-expressing tumors cells in in vitro experiments and in vivo in mice [30], yet only a comparatively small fluorescence quantum yield. To improve the sensitivity of this otherwise high potential modular probe, we are currently investigating possible fluorescence quenching pathways and are looking for alternative labels. In the present work, we have studied systematically the spectroscopic and pharmacological properties of a series of recently introduced, commercial asymmetric cyanines, the dyes DY-681, DY-731, DY-751, and DY-776, in comparison to DY-676 and clinically approved ICG. The aim was here to identify better suitable fluorophores with red shifted absorption and emission bands and high fluorescence quantum yields in aqueous solution and in a model body fluid, low unspecific binding as well as high stability and low cytotoxicity.

2. Results and discussion

2.1. Absorption and fluorescence study of the target-specific model bioconjugate of DY-676

Electronic absorption and fluorescence spectroscopy are universally employed to characterize fluorescent labels and probes. Application-relevant parameters determined with these techniques include the spectral position of the absorption (abs) and emission (em) bands, the band widths (FWHM: full width at half-height of the maximum) that can e.g. provide a hint for dye aggregation in the case of absorption [11,31,32], the Stokes shift [10], that determines the ease of separating separation of excitation from emission and the signal collection efficiency, the molar absorption coefficient ε and the fluorescence quantum yield Φ_f. The product of ε (at the excitation wavelength) and Φ_f, that is often termed brightness, determines the sensitivity from the dye-side [10]. A maximized sensitivity is relevant e.g. for applications such as detecting metastatic spread of a tumor [18]. FabAntiCEA—DY-676 and, less pronounced also DY-676, reveal an enhanced absorption blue-shifted from the dye's main absorption band and apparent spectral broadening in phosphate buffered saline (PBS) [33] in comparison to PBS with 5% (w/v) bovine serum albumin (BSA; PBS/BSA) modeling body fluid (Fig. 1, top and Table 1), whereas the corresponding fluorescence emission spectra (Fig. 1, bottom) and excitation spectra in PBS and PBS/BSA (not shown) match. The fluorescence quantum yield of the nonconjugated dye always considerably exceeds that of FabAntiCEA—DY-676 (Table 1). Similar effects have been observed for other DY-676 bioconjugates, e.g. FabIgG—DY-676. The presence of BSA results in a fluorescence enhancement of 7.8 and 5 for DY-676 and FabAntiCEA—DY-676, respectively (Table 1), yet the Φ_f value of the free dye considerably exceeds that of bioconjugated DY-676.

The appearance of this enhanced absorption band blue-shifted from the main dye absorption maximum, in conjunction with the unaffected fluorescence spectra, suggests the formation of dye aggregates, most likely nonfluorescent H-type dimers [11,34–37]. This can most likely explain the only moderate fluorescence quantum yields of DY-676 and especially of FabAntiCEA—DY-676 in PBS. A similar reduction in fluorescence has been reported e.g. for Cy5 upon covalent linkage to antibodies like IgG, [38,39]. The strong enhancement in emission in conjunction with the red shift in the absorption maximum in the presence of BSA observed for DY-676 points to dye–BSA interactions. Dye–protein interactions have been reported also for other cyanine dyes [40], that are, however, often accompanied by stronger spectral shifts in absorption and in emission [40,41]. Dye–protein interactions may also account for the

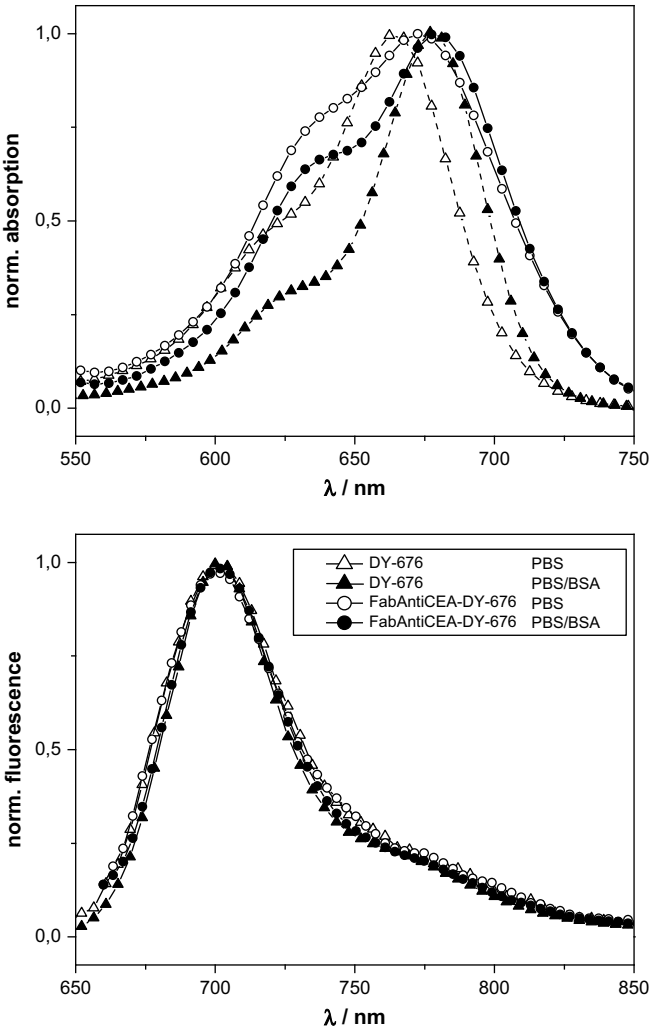

Fig. 1. Spectroscopic characterization of bioconjugated and non-conjugated DY-676. Normalized absorption (top) and normalized fluorescence emission (bottom) spectra of FabAntiCEA—DY-676 in comparison to DY-676 in PBS and in PBS/BSA (5 mass-% albumin BSA in PBS; w/v) solution.

Table 1
Spectroscopic properties of FabAntiCEA—DY-676 in PBS and PBS/BSA in comparison to nonconjugated DY-676. Maxima of the main absorption (λ_{abs}) and emission (λ_{em}) bands and fluorescence quantum yields (Φ_f).

Dye	Solvent	λ_{abs}/nm	λ_{em}/nm	Φ_f
DY-676	PBS	664	702	0.04
DY-676	PBS/BSA	676	702	0.31
FabAntiCEA-DY-676	PBS	675	702	0.01
FabAntiCEA-DY-676	PBS/BSA	680	702	0.05

increase of Φ_f of FabAntiCEA—DY-676 in PBS/BSA. The smaller enhancement factor (FEF) of bioconjugated DY-676 as compared to unbound DY-676 suggests either weakened dye–BSA interactions or that not all the antibody-attached DY-676 fluorophores are accessible to BSA.

2.2. Absorption and fluorescence study of the new DY dyes in comparison to ICG and DY-676

The search for a substitute for DY-676 revealed distinct spectroscopic properties of the recently developed DY dyes shown in Fig. 2 in comparison to DY-676 and ICG. These dyes, which all carry the same indole end group, equipped with two negatively charged sulfonate groups to promote water solubility, were chosen to differ in the chemical nature of the aromatic benzopyrylium-type end group (acceptor strength, planarity, rigidity) and in the length of the polymethine chain. DY-681 differs from the other DY dyes with respect to the position of the oxygen atom of the benzopyrylium end group and the polymethine chain. DY-681 reveals ortho attachment and the other dyes attachment at the para position.

The DY dyes display absorption bands between 660 nm and 780 nm in PBS and PBS/BSA matching typical laser diodes and emission maxima between 700 nm and 800 nm, respectively (Fig. 3), due to cyanine-type optical transitions delocalized over the whole π-conjugated system. DY-681 and DY-751 are potential substitutes for the common fluorescent labels Cy5.5 and Cy7. The molar absorption coefficients (at the dyes' main absorption maximum) of the DY dyes are in the order of 80,000–170,000 L mol^{-1} cm^{-1} in PBS/BSA. The spectral position of their absorption and emission bands following the order of DY-676 < DY-681 < DY-731 < DY-751 < DY-776 < ICG (Fig. 3 and Table 2) is determined by the length of the polymethine chain and the electron density at the benzopyrylium-type end group, that increases in the order of DY-731 < DY-751 < DY-776 for the pentamethine dyes [21,42]. Intriguingly with respect to the desired application are the red absorption and emission bands of the trimethine dyes DY-676 and DY-681 and the pentamethine DY dyes in comparison to known symmetric cyanine dyes of similar polymethine chain length and to the heptamethine ICG. This underlines the great effective length of the benzopyrylium-type end groups of the DY dyes [21,43]. The realization of long wavelength absorption and emission bands with a minimum number of conjugated double bonds can be advantageous for the design of NIR-excitable fluorophores with high fluorescence quantum yields and high stability, as for cyanine dyes, rotations around single bonds in the polymethine chain and excited state cis–trans isomerization of flexible double bonds are common pathways for the nonradiative deactivation of the excited singlet state[18,21,44]. These processes, that become increasingly likely with increasing number of flexible double bonds, can also hamper the photochemical stability of cyanine dyes. As follows from Fig. 4, the fluorescence quantum yields of the DY dyes in PBS and PBS/BSA exceed considerably that of ICG except for DY-676 and DY-776 in PBS. In addition, all the DY dyes reveal a larger Stokes shift than ICG with the highest values of 804 cm^{-1} and 570 cm^{-1} found for DY-676 in PBS and for DY-731 in PBS/BSA (Table 2), respectively.

Relevant information determining the suitability of the DY dyes for the desired application follows from the size of the dyes' fluorescence quantum yields in PBS and the observation of spectral broadening in absorption or the appearance of extra absorption bands in PBS as well as from the influence of BSA on the spectroscopic properties of the DY dyes. Particularly the spectral position

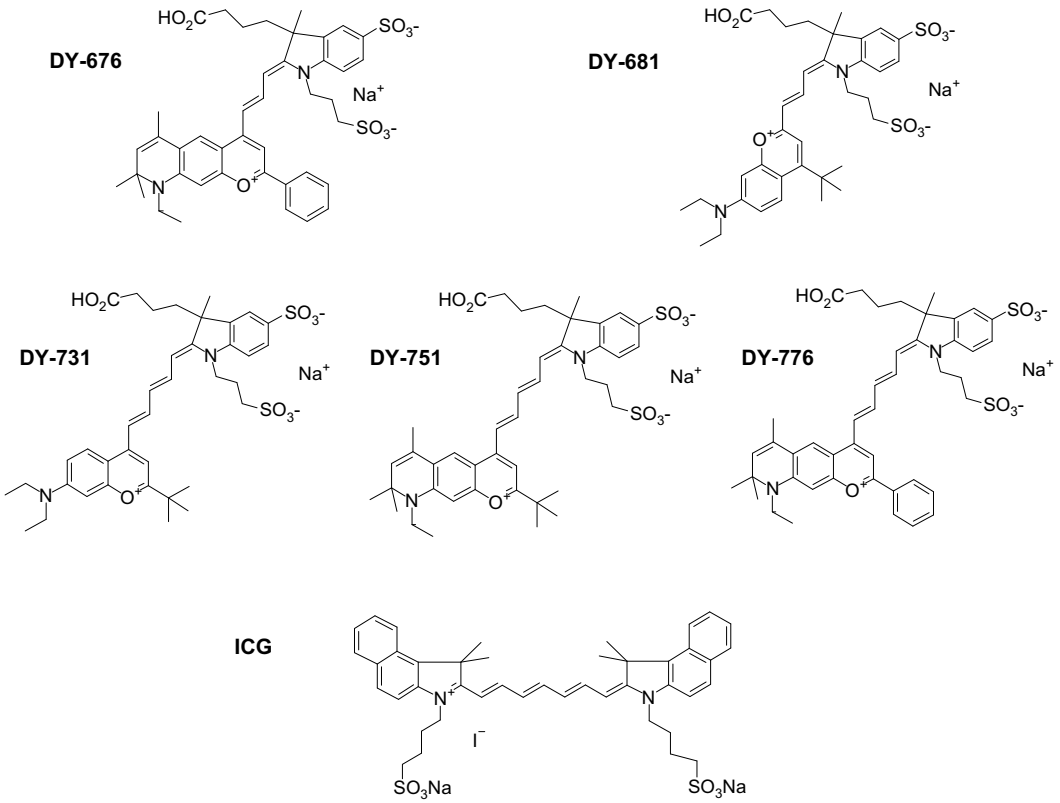

Fig. 2. Chemical structures of the studied cyanines. Asymmetric trimethine dyes DY-676 and DY-681 (top), asymmetric pentamethine dyes DY-731, DY-751, and DY-776 (middle), and clinically approved symmetric heptamethine dye ICG (bottom).

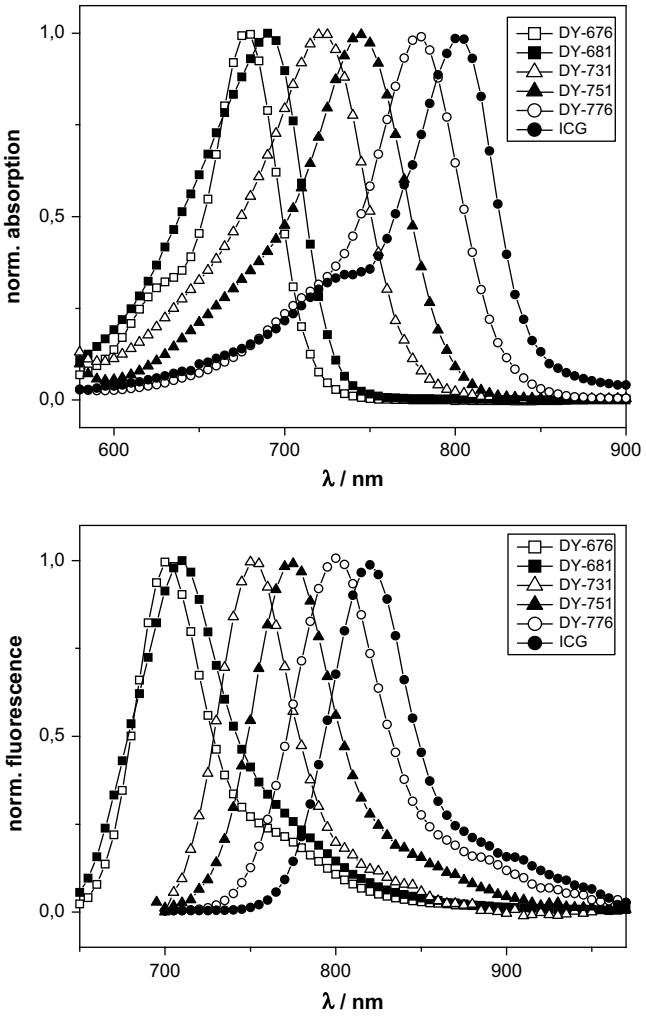

Fig. 3. Spectroscopic characterization of the studied cyanines. Normalized absorption (top) and normalized emission (bottom) spectra of the DY-dyes DY-681, DY-731, DY-751, and DY-776 in PBS/BSA in comparison to DY-676 and ICG.

Table 2
Spectroscopic properties of the DY dyes in PBS and PBS/BSA in comparison to DY-676 and ICG. Maxima of the main absorption (λ_{abs}) and emission (λ_{em}) bands, bandwidth ($FWHM_{abs}$, FWHM: full width at half-height of the maximum), for a better comparison of the dyes given on an energy scale (cm^{-1}), Stokes shift, fluorescence quantum yields (Φ_f), and BSA-induced fluorescence enhancement factor (FEF). The Stokes shift is the energetic difference between the spectral position of the lowest energy (that is, the longest wavelength) absorption maximum and the spectral position of the lowest energy emission band and is accordingly typically provided on an energy scale. The differences between the absorption maximum in PBS and the absorption maximum in PBS/BSA on a better comparable energy scale are: DY-676: 300 cm^{-1}, DY-681: 224 cm^{-1}, DY-731: 68 cm^{-1}, DY-751: 211 cm^{-1}, DY-776: 287 cm^{-1}, ICG: 376 cm^{-1}.

Dye	Solvent	λ_{abs}/nm	$FWHM_{abs}/cm^{-1}$	λ_{em}/nm	Stokes shift/cm^{-1}	Φ_f	FEF
DY-676	PBS	664	1505	702	804	0.04	
DY-676	PBS/BSA	678	1009	702	504	0.31	7.8
DY-681	PBS	679	1603	712	700	0.11	
DY-681	PBS/BSA	690	1627	710	397	0.40	3.6
DY-731	PBS	718	1527	752	630	0.10	
DY-731	PBS/BSA	722	1491	755	570	0.30	3.0
DY-751	PBS	734	1473	770	622	0.10	
DY-751	PBS/BSA	744	1315	775	512	0.24	2.4
DY-776	PBS	756	1946	796	538	0.01	
DY-776	PBS/BSA	776	1025	799	376	0.10	10
ICG	PBS	780	1011	810	514	0.04	
ICG	PBS/BSA	807	973	822	258	0.08	2.0

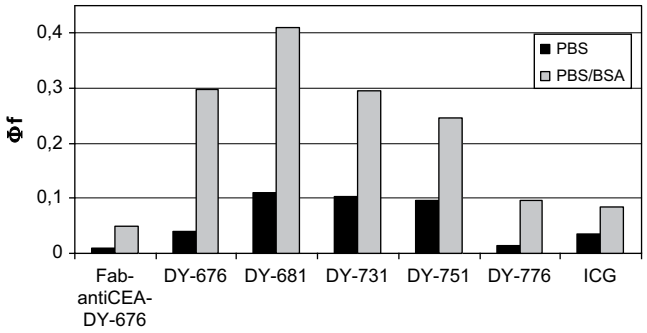

Fig. 4. Comparison of the fluorescence efficiency of the studied cyanines. Fluorescence quantum yields (Φ_f) of the evaluated DY dyes in PBS and in PBS/BSA in comparison to DY-676 and ICG and to FabAntiCEA—DY-676.

of the absorption maximum, the molar absorption coefficient, the width of the absorption band, and the fluorescence quantum yields of the DY dyes and ICG are affected by BSA (Table 2 and Fig. 4). In all cases, the absorption maxima are red shifted in the presence of BSA as compared to PBS, with the smallest shift of 4 nm (equaling 68 cm^{-1} on an energy scale, that provides a better comparability of spectral data covering a broader wavelength range, see also Table 2) being displayed by DY-731. A sizeable shift in emission occurs only for ICG. Such bathochromic shifts in the absorption maxima of cyanine dyes are observed frequently in conjunction with a decrease in polarity of the fluorophore local environment [11,40,41]. Assuming that the size of the BSA-induced spectral changes is mainly determined by dye hydrophilicity, this points to ICG as the least hydrophilic dye among the series of fluorophores studied followed by DY-676 and DY-776 (Table 2).

The fluorescence quantum yields of the DY dyes and ICG in PBS and PBS/BSA, see Table 2, are determined by the interplay of different effects: i.) rotations around single bonds in the polymethine chain and excited state cis–trans isomerization of flexible double bonds that typically presents the main nonradiative deactivation pathway of this class of chromophores [21,44–46] and ii.) the formation of (nonfluorescent) aggregates [21], that is significantly affected by dye charge and hydrophilicity [45–48]. For the red emitting dyes of the series studied, also iii.) the so-called energy gap rule can play a role [21,49,50]. This rule predicts an increase of the nonradiative rate constant (enhanced internal conversion), and thus reduced fluorescence quantum yields with a narrowing of the S_1–S_0 energy gap. For the fluorophores compared, a considerable influence of solvent viscosity rigidizing flexible molecules and thereby influencing i.) [21,44] seems not very likely in the case of PBS/BSA, as this should similarly affect all the dyes studied. The formation of nonfluorescent aggregates seems to be mainly responsible for the low fluorescence quantum yields of DY-676 and DY-776 in PBS as suggested by the enhanced short-wavelength absorption and pronounced spectral broadening found especially in PBS (Fig. 1 and Table 2). Both dyes are equipped with the same *N*-bridged benzopyrylium entity that, among the DY dyes studied, seems to favor π–π-interactions between adjacent dye molecules [42]. Replacement of the phenyl group of the *N*-bridged benzopyrylium entity by a tert-butyl group (DY-751) or incorporation of a smaller benzopyrylium moiety with tert-butyl and diethylamino substituents (DY-681, DY-731) results in comparatively high fluorescence quantum yields of *ca.* 0.1 in PBS. The Φ_f values of DY-681, DY-731, and DY-751 reach e.g. the Φ_f values reported for certain hydrophilic glucamine- and glucosamine-substituted cyanines in aqueous solution [3,8,21,48,51–53]. One factor contributing to the improved fluorescence quantum yields of these three dyes in aqueous solution could be a reduced aggregation tendency.

Table 3
Photometrically determined thermal stability of the DY dyes in PBS and PBS/BSA after 3 days (d) of storage at 4 °C and 37 °C in comparison to DY-676 and ICG. The dye concentration was always 1×10^{-6} mol/L.

Dye	Absorption intensities relative to starting value in %			
	PBS	PBS	PBS/BSA	PBS/BSA
	3 d, 4 °C	3 d, 37 °C	3 d, 4 °C	3 d, 37 °C
DY-676	96	91	98	100
DY-681	95	93	94	96
DY-731	90	80	87	93
DY-751	94	82	86	82
DY-776	95	90	101	97
ICG	66	31	96	84

Mainly responsible for the generally observed fluorescence enhancement in the presence of BSA seems to be a BSA-binding-induced rigidization of the dye molecules, reducing rotations around single bonds in the polymethine chain and excited state cis–trans isomerization, most likely in combination with the prevention of dye aggregation in the case of DY-676 and DY-776, that display the strongest enhancement factors, see Table 2. The size of these dye–BSA interactions is dye-dependent. Among the dyes studied, DY-681 and especially the red emitting fluorophores DY-731 and DY-751, that reveal the highest quantum yields in PBS and the smallest BSA-induced changes in absorption and emission, are the best suited candidates for the application as fluorescent labels in target-specific probes for NIRF imaging.

2.3. Thermal stability

In order to cover the systemic interrelations of contrast agents, in vivo NIRF imaging studies are commonly performed over one to two days. Accordingly, imaging reagents must be sufficiently stable. This has to be clarified under conditions modeling the in vivo situation prior to use in an animal model. As follows from Table 3, all the DY dyes show a considerably improved thermal stability in PBS after 72 h of storage at 4 °C and 37 °C as compared to ICG with relative intensities between 90% and 96% for 4 °C (ICG: 66%) and 80% and 93% for 37 °C (ICG: 31%), respectively, in comparison to the situation immediately after dissolution (100%). In PBS/BSA, the stability of the DY dyes is also very high with values between 86% and 100% for 4 °C in comparison to ICG (96%). In PBS/BSA at 37 °C, which approximates the in vivo situation by the presence of albumin and the use of body temperature, DY-676, DY-681, DY-776, and DY-731 display an improved stability (93–100%) with respect to ICG (84%). Only the stability of DY-751 (82%) is similar to that of ICG. In all cases, comparable results followed from the corresponding emission studies not shown here.

The increased stability of ICG in protein-containing solutions has been previously described [25,27] and is attributed to a protein-binding-induced stabilization [25,26]. In contrast, for the DY dyes showing a high stability both in PBS and BSA/PBS, the presence of the protein plays only a minor role. The most important factor governing dye stability seems to be the generally shorter polymethine chains of the DY dyes. This improved stability of the DY dyes DY-676, DY-681, DY-776 and DY-731 under in vivo approximating conditions is advantageous for the applicability as in vivo diagnostic agents.

2.4. Cytotoxicity

A stringent requirement for the application of fluorophores in vivo experiments is a low cytotoxicity. Cytotoxicity studies were therefore performed on a macrophage and an endothelial cell line measuring the cell vitality after incubation with the fluorescent label to be tested e.g. via a so-called dead-or-alive assay. Cell lines suitable for modeling the in vivo NIRF situation in the vascular system are macrophage cells and murine endothelial cells because of the extensive contact of these cells with intravenously applied substances. Despite the relevance for the choice of suitable fluorescent reporters for in vivo fluorescence imaging and their strong

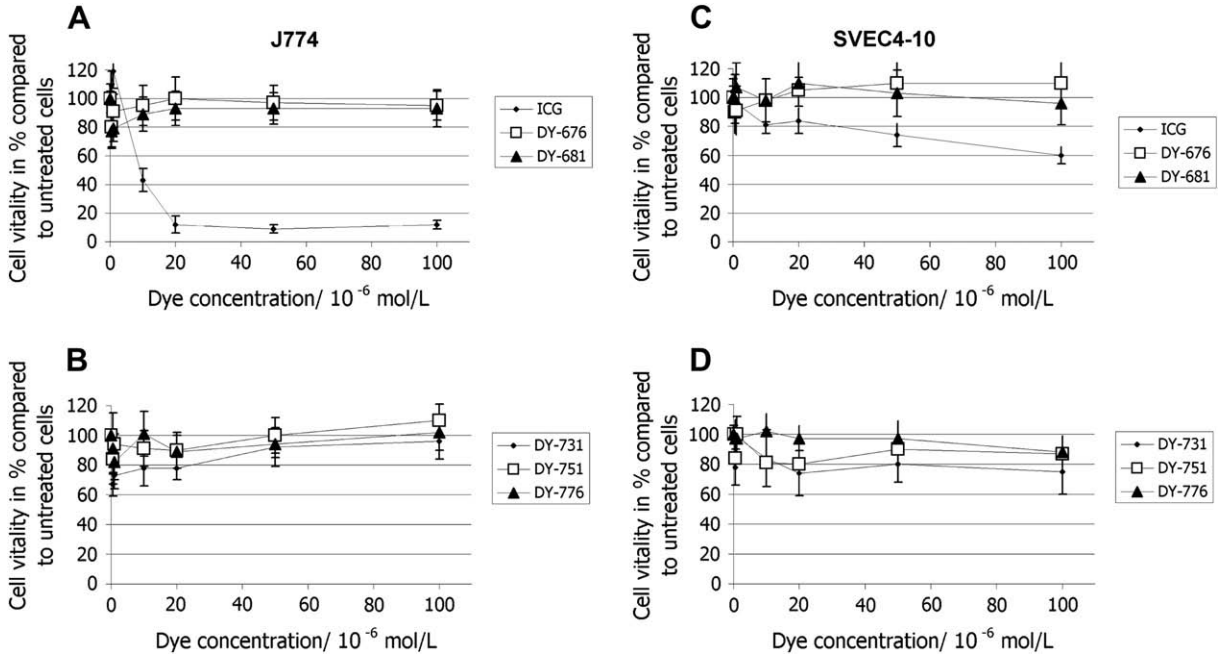

Fig. 5. Comparison of the cytotoxicity of the studied cyanines. Cytotoxicity of the DY dyes and ICG determined for a mouse macrophage cell line (J774; panels A and B) and an endothelial (SVEC4-10; panels C and D) cell line after 72 h of incubation with each dye. Cell cultures without any dye treatment exhibit a cell vitality of 100%. The lines are only guide to the eye.

impact on the cytotoxicity of targeted probes and contrast agents, to the best of our knowledge, aside from clinically approved ICG [27–29], data on the cytotoxicity of fluorescent dyes are scarcely available [54].

As follows from Fig. 5, the DY dyes generally show very low cytotoxic effects on both macrophages (Fig. 5, panels A and B) and endothelial cells (Fig. 5, panels C and D). For an incubation time of 72 h at the maximum tested dye concentration of 100×10^{-6} mol/L, the macrophage cell vitality is 93% in the case of DY-681 and DY-676 and 96% in the case of DY-731 compared to untreated cells (100%). DY-751 and DY-776 demonstrate no cytotoxicity at all with cell vitality values slightly over 100%. When incubating endothelial cells with DY dyes, the strongest cytotoxic effects result for DY-731 (cell vitality of 75%) and the smallest for DY-676 (cell vitality over 100%) and DY-681 (cell vitality of 96%). For the DY fluorophores, dye concentration and cytotoxicity do not correlate. Surprisingly, for both cell types, the strongest cytotoxic effects are found for clinically approved ICG. A considerable reduction of the macrophage cell vitality is observed already at an ICG concentration of 10×10^{-6} mol/L after 72 h. The vitality decreases steadily with increasing dye concentration and reached a value of 12% at the maximum tested dye concentration of 100×10^{-6} mol/L (Fig. 5, panel A). Compared to macrophages, ICG cytotoxicity on endothelial cells is lower, with a remaining cell vitality of 60% after 72 h resulting in an ICG concentration of 100×10^{-6} mol/L (Fig. 5, panel C).

The very advantageous fact that the DY dyes studied generally exhibit significantly lower cytotoxic effects for both macrophage and endothelial cells, but especially for macrophage cells at high dye concentration, could be related to their reduced lipophilicity/increased hydrophilicity as compared to ICG. A straightforward relationship between lipophilicity and cytotoxic effects has been revealed previously [55,56]. For example, Cascorbi et al. found a direct correlation between lipophilicity and cytotoxicity for yeast cells [56]. The cytotoxic effects observed by us for ICG particularly on macrophage cells and, less pronounced, for endothelial cells, agree with the results from other groups that also reported a considerable cytotoxicity of ICG in vitro [27,28,57] and in vivo [27–29]. Enaida et al. for example demonstrated with rat eyes, that after intravitreous ICG application, the retinal function was impaired even by low doses of ICG (0.025 g/L) [57]. Higher doses of ICG (25 g/L) completely destroyed the normal structure of the retina. The most probable mechanism for cell damage by ICG is an effect on mitochondrial enzyme activity leading to apoptosis [28]. However, other mechanisms could be involved as well [28]. The stronger cytotoxic effects on macrophage cells in comparison to endothelial cells are ascribed to differences in uptake as has been previously discussed for the dye Nile blue A [54].

3. Conclusion

In summary, all the tested trimethine and pentamethine DY dyes exhibit comparatively red shifted absorption and emission bands, enhanced fluorescence quantum yields, a better thermal stability, and a clearly reduced cytotoxicity in comparison to clinically established ICG. The size of the fluorescence quantum yield of the DY dyes in aqueous solution is primarily dependent on the substitution pattern of the benzopyrylium-type end group which notably determines the aggregation tendency. With DY-681 and especially with the NIR-excitable, red emitting dyes DY-731 and DY-751, we identified new attractive diagnostic tools for in vitro and in vivo fluorescence applications. In the case of the DY-676 bioconjugates targeted against carcinoembryonic antigen (CEA)-expressing tumor cells, dye aggregation was identified as a major source for the only moderate fluorescence quantum yields in PBS and BSA/PBS. Substitution of DY-676 for DY-681, DY-731 and DY-751 is expected to yield similarly selective, yet considerably more fluorescent probes and thus improved limits of detection in conjunction with an increased depth of penetration in the case of DY-731 and DY-751 due to the red shifted absorption and emission bands. These findings present an important advance toward new and comparatively less expensive tools of known stability and cytotoxicity for NIRF imaging. In addition, these results clearly reveal the importance of known structure–property relationships for the choice of optimum fluorophores.

4. Experimental

4.1. Apparatus and reagents

The absorption spectra were recorded on a CARY 5000 spectrometer (Varian Inc., Palo Alto, USA). The fluorescence emission and fluorescence excitation spectra were measured with a Spectronics Instruments 8100 (Westbury, USA). For the cytotoxicity studies, a microplate reader from Molecular Devices, CA, USA was used.

Indocyanine green (ICG) was purchased from Pulsion Medical Systems AG (München, Germany). The DY dyes DY-676, DY-681, DY-731, DY-751, and DY-776 were provided by Dyomics GmbH (Jena, Germany). The purity of the fluorescent dyes was at least 90% according to the specification of the manufacturer. The dyes IR 125 and Oxazine 1 used as fluorescence quantum yield standards were obtained from Lambda Physik GmbH (Goettingen, Germany). All the organic solvents used, i.e., DMSO, DMF, and ethanol, were of spectroscopic grade and purchased from Sigma Aldrich. Phosphate buffered saline solution (PBS, 7.7×10^{-4} mol/L, pH 7.4) was obtained from GIBCO Life Sciences (Paisley, Scotland) and bovine serum albumin (BSA; fraction V) from Merck KgaA (Darmstadt, Germany). Dulbecco's Modified Eagle's Medium (DMEM) and heat inactivated fetal calf serum (FCS) used for the preparation of the cell culture medium were both purchased from Gibco/Invitrogen (Karlsruhe, Germany) and from Gibco BRL Life Technologies (Paisley, Scotland). The murine endothelial cells (SVEC4-10) and the macrophage cells (J774) used for the cytotoxicity studies were obtained from DSMZ (Braunschweig, Germany) and ATCC Biomaterials (Wesel, Germany). The tetrazolium salt MTS (CellTiter96®) employed for the determination of the cell vitality was obtained from Promega GmbH (Mannheim, Germany). The microtiter plates used were from Greiner Bio-One GmbH (Frickenhausen, Germany).

DY-676 conjugates of a specific Fab antibody fragment directed against the carcinoembryonic antigen CEA (arcitumomab®) [58] available from CEA-Scan, Immunomedics (Darmstadt, Germany) and DY-676 conjugates of a nonspecific Fab antibody fragment generated from mouse IgG by Dianova (Hamburg, Germany) referred to as FabAntiCEA—DY-676, were obtained as previously described [30] in accordance to the manufacturer's protocol, incubating DY-676 *N*-hydroxysuccinimidyl (NHS) esters with the respective protein in phosphate buffered saline (PBS, 1×10^{-1} mol/L, pH 9.3). The dye-labeled protein was separated from unbound fluorophore by sephadex gel filtration (Amersham Biosciences, Uppsala, Sweden). The dye-to-protein ratio of the FabAntiCEA—DY-676 shown here was determined to 4:1 from measurements of the absorbances at 280 nm and 660 nm according to Mujumdar et al. [59].

4.2. Absorption measurements

The absorption spectra of the DY dyes, their bioconjugates, and ICG were determined in duplicate in a PBS solution (7.7×10^{-4} mol/L, pH 7.4) and in PBS containing 5 mass-% (w/v) BSA (PBS/BSA) at

a dye (or species) concentration of 1×10^{-6} mol/L. The molar absorption coefficients of each dye at the dye's absorption maximum $\varepsilon(\lambda_{max})$ were determined from three independent measurements of the absorption spectra of single diluted stock solutions in PBS and BSA/PBS, yet not from a concentration series. The bandwidth of the absorption bands ($FWHM_{abs}$: full width at half-height of the absorption maximum) was determined on an energy scale for a better comparison of the dyes differing in the spectral position of their absorption bands.

4.3. Fluorescence measurements

The fluorescence experiments were performed with a Spectronics Instruments 8100 (Westbury, USA) spectrofluorometer (T-type design with UV/vis and vis/NIR detection channels with the NIR emission channel used here consisting of a single monochromator and a silicon avalanche photodiode) equipped with Glan Thompson polarizers and calibrated with physical transfer standards according to previously described procedures [60]. Typically, the emission was excited at the blue vibronic shoulder of the longest wavelength absorption band (absorbances of 0.02–0.06 to minimize inner filter effects and reabsorption). The emission spectra of the DY dyes, their bioconjugates, and ICG were determined in duplicate in PBS and in PBS/BSA at a dye (or species) concentration of 1×10^{-6} mol/L. For selected samples, also the excitation spectra were measured that represent the absorption spectra of the emitting species.

For the measurement of the fluorescence quantum yields (ϕ_f) of the dyes employing the laser dye IR 125 in DMSO and Oxazine 1 in ethanol as fluorescence standards, Glan Thompson polarizers placed in the excitation and the emission channels were set to 0° and 54.7°, respectively. For each compound–solvent pair, the quantum yields were determined in duplicate using dye and standard solutions freshly prepared upon dilution of stock solutions (typical dye concentration of 100×10^{-6} mol/L, solvent DMF, stored in the refrigerator at 4 °C in the dark).

To remove instrument-specific distortions from the measured fluorescence data, the fluorescence emission spectra were corrected for the wavelength- and polarization-dependent spectral responsivity of the detection system traceable to the spectral radiance scale [60]. The emission spectra on a wavenumber or energy scale were obtained by multiplying the measured and corrected emission spectra on a wavelength scale with λ^2 [61]. The ϕ_f values of the DY series, ICG, and FabAntiCEA—DY-676 were calculated from integrated, blank, and spectrally corrected emission spectra (wavelength scale; prior to integration multiplication with λ) relative to the standards IR 125 and Oxazine 1 using the following formula [62,63]:

$$\phi_{f,x} = \phi_{f,st} \times \frac{F_x}{F_{st}} \times \frac{f_{st}(\lambda_{ex})}{f_x(\lambda_{ex})} \times \frac{n_x^2}{n_{st}^2} \quad (1)$$

Here, $f(\lambda_{ex})$ is the absorption factor at the excitation wavelength λ_{ex} that is equivalent to the formerly used absorptance $\alpha(\lambda_{ex})$ [64]. $f(\lambda_{ex})$ is nonlinearly linked to the absorbance $A(\lambda_{ex})$ $f(\lambda_{ex}) = 1 - 10^{-A(\lambda_{ex})} = 1 - 10^{-\varepsilon(\lambda_{ex})cl}$ with ε equaling the molar decadic absorption coefficient, c the chromophore concentration, and l the optical pathlength) [60]. F is the integral emission intensity, i.e., the area under the blank and spectrally corrected emission spectrum on a wavelength scale, and n the refractive index of the solvent(s) used. The subscripts x and st denote sample and standard (IR 125 in DMSO: $\phi_{f,st} = 0.22$; Oxazine 1 in ethanol: $\phi_{f,st} = 0.15$). No attempts were made to correct the measured absorption intensities for contributions from nonfluorescent species. In these cases (e.g. DY-676, DY-776, and FabAntiCEA—DY-676 in PBS), the given ϕ_f values equal only the fluorescence quantum yield of the solution and not the fluorescence quantum yield of the emitting species. Typical uncertainties (standard deviations) of fluorescence quantum yield measurements as derived from previous experiments (six replicates) are ±5% (for $\phi_f > 0.4$), ±10% (for $0.2 > \phi_f > 0.02$), ±20% (for $0.02 > \phi_f > 0.005$), and ±30% (for $0.005 > \phi_f$), respectively [65].

4.4. Thermal stability

The thermal stability of the NIR chromophores was determined from the absorption spectra of the dyes in PBS and in BSA/PBS (dye concentration 1×10^{-6} mol/L) at 4 °C and at 37 °C, respectively, for a diagnostically relevant time domain of up to 72 h. For the data evaluation, the absorption intensities were taken from the main absorption maximum with the values for the fresh solutions (0 h) being set to 100%. To ensure that changes in absorption intensity correlate with changes in dye concentration, all the samples were controlled gravimetrically to account for loss of solvent. Typical uncertainties (standard deviation from six replicates) of absorption measurements with transparent dilute solutions in this intensity range are ±2% [66]. The thermal stabilities of FabAntiCEA—DY-676 and DY-676 conjugated to a nonspecific IgG antibody fragment have been previously reported [30].

4.5. Cytotoxicity

Dye cytotoxicity was determined for both murine endothelial cells (SVEC4-10) and macrophage cells (J774) in culture. These particular cell lines were chosen because of the extensive contact of endothelial cells and macrophages with intravenously applied substances. The cells were grown in DMEM containing 10% (v/v) of heat inactivated fetal calf serum at 37 °C, 10% CO_2, and a relative humidity of 95%. The cell cultures were routinely assessed for contamination with mycoplasms. For the determination of the cytotoxicity, the cells were seeded in microtiter plates and incubated with different concentrations of the DY dyes or ICG (concentrations: 0.5×10^{-6} mol/L, 1×10^{-6} mol/L, 10×10^{-6} mol/L, 20×10^{-6} mol/L, 50×10^{-6} mol/L, 100×10^{-6} mol/L) between 24 and 72 h. The cell vitality was obtained from measurements of the activity of cellular dehydrogenase in dye-treated and nontreated cells after addition of the tetrazolium salt MTS (20×10^{-6} L per well, 1.9 g/L MTS). Living cells turned MTS into a blue formazan product, the concentration of which was determined photometrically from the absorption at 492 nm after an incubation time of 1 h using a microplate reader. The formazan concentration is directly proportional to the number of living cells in the respective cell culture. The cell viability was expressed in relative numbers in relation to untreated controls. Values lower than 100% indicate cytotoxicity, higher values cell proliferation. The test was performed six times for each dye concentration and cell line. The cytotoxicity of FabAntiCEA—DY-676 and DY-676 conjugated to a nonspecific FabIgG antibody fragment have been previously reported [30].

Acknowledgement

We thank Marcus-Rene Lisy, PhD and Melanie Kettering, PhD, IDIR, Jena for assistance in the stability and cytotoxicity studies.

References

[1] C. Bremer, V. Ntziachristos, U. Mahmood, C.H. Tung, R. Weissleder, Radiologe 41 (2001) 131–137.
[2] V. Ntziachristos, J. Ripoll, L.V. Wang, R. Weissleder, Nat. Biotechnol. 23 (2005) 313–320.
[3] K. Licha, Top. Curr. Chem. 222 (2002) 1–29.
[4] G.A. Wagnières, W.M. Star, B.C. Wilson, Photochem. Photobiol. 68 (1998) 603–632.

[5] N.M. Marin, N. MacKinnon, C. MacAulay, S.K. Chang, E.N. Atkinson, D. Cox, D. Serachitopol, B. Pikkula, M. Follen, R. Richards-Kortum, J. Biomed. Opt. 11 (2006) 014010-1–014010-14.
[6] E.C. Bradley, J.W. Barr, Life Sci. 7 (1968) 1001–1007.
[7] F.J. Klocke, D.G. Greene, R.C. Koberstein, Circ. Res. 22 (1968) 841–853.
[8] R.C. Benson, H.A. Kues, Phys. Med. Biol. 23 (1978) 159–163.
[9] C.M. Leevy, F. Smith, J. Longueville, JAMA 200 (1967) 236–240.
[10] U. Resch-Genger, M. Grabolle, S. Cavaliere-Jaricot, R. Nitschke, T. Nann, Nat. Meth. 5 (2008) 763–775.
[11] S.A. Hilderbrand, R. Weissleder, C.H. Tung, Bioconjugate Chem. 16 (2005) 1275–1281.
[12] A. Hansch, O. Frey, I. Hilger, D. Sauner, M. Haas, D. Schmidt, C. Kurrat, M. Gajda, A. Malich, R. Bräuer, W.A. Kaiser, Invest. Radiol. 39 (2004) 626–632.
[13] I. Hilger, Y. Leistner, A. Berndt, C. Fritsche, K.M. Haas, H. Kosmehl, W.A. Kaiser, Eur. Radiol. 14 (2004) 1124–1129.
[14] E.M. Sevick-Muraca, J.P. Houston, M. Gurfinkel, Curr. Opin. Biol. 6 (2002) 642–650.
[15] C. Bremer, V. Ntziachristos, B. Weitkamp, G. Theilmeier, W. Heindel, R. Weissleder, Invest. Radiol. 40 (2005) 321–327.
[16] R. Weissleder, V. Ntziachristos, Nat. Med. 9 (2003) 123–128.
[17] B. Ballou, B.C. Lagerholm, L.A. Ernst, M.P. Bruchez, A.S. Waggoner, Bioconjugate Chem. 15 (2004) 79–86.
[18] J.L. Kovar, M.A. Simpson, A. Schutz-Geschwender, D.M. Olive, Anal. Biochem. 367 (2007) 1–12.
[19] B. Ballou, L.A. Ernst, A.S. Waggoner, Curr. Med. Chem. 12 (2005) 795–805.
[20] K.E. Adams, S.I. Ke, S. Kwon, F. Liang, Z. Fan, Y. Lu, K. Hirschi, M.E. Mawad, M.A. Barry, E.M. Sevick-Muraca, J. Biomed. Opt. 12 (2007) 024017-1–024017-9.
[21] S. Stoyanov, Probes: dyes fluorescing in the NIR region, in: R. Raghavachari (Ed.), Near-infrared Applications in Biotechnology, Marcel Dekker Inc, New York. PA, 2001, pp. 35–93.
[22] S.A. Soper, Q.L. Mattingly, J. Am. Chem. Soc. 116 (1994) 3744–3752.
[23] T.J. Muckle, Biochem. Med. 15 (1976) 17–21.
[24] E.D. Moody, P.J. Viskari, C.L. Colyer, J. Chromatogr. B. Biomed. Sci. Appl. 729 (1999) 55–64.
[25] J. Gathje, R. Steuer, K.R. Nicholes, J. Appl. Physiol. 29 (1976) 181–185.
[26] M.L.J. Landsman, G. Kwant, G.A. Mook, W.G. Zijlstra, J. Appl. Physiol. 40 (1976) 575–583.
[27] J.D. Ho, R.J. Tsai, S.N. Chen, H.C. Chen, Arch. Ophthalmol. 121 (2003) 1423–1429.
[28] H. Ikagawa, M. Yoneda, M. Iwaki, Z. Isogai, K. Tsujii, R. Yamazaki, T. Kamiya, M. Zako, Ophthalmol. Vis. Sci. 46 (2005) 2531–2539.
[29] K. Skrivanova, J. Skorpikova, J. Svihalek, V. Mornstein, R. Janisch, J. Photochem. Photobiol., B 85 (2006) 150–154.
[30] M.-R. Lisy, A. Goermar, C. Thomas, J. Pauli, U. Resch-Genger, W.A. Kaiser, I. Hilger, Radiology 247 (2008) 779–787.
[31] W.G. Cox, M.P. Beaudet, J.Y. Agnew, J.L. Ruth, Anal. Biochem. 331 (2004) 243–254.
[32] C.M. Soto, A.S. Blum, G.J. Vora, N. Lebedev, C.E. Meador, A.P. Won, A. Chatterji, J.E. Johnson, B.R. Ratna, J. Am. Chem. Soc. 128 (2006) 5184–5189.
[33] No attempts were made to separate the main red absorption band and the blue-shifted band via spectral fitting. The presence of two close lying non-separated bands can also result in apparent spectral broadening.
[34] W. West, S. Pearce, J. Phys. Chem. 69 (1965) 1894–1903.
[35] A.H. Herz, Photogr. Sci. Eng. 18 (1974) 323–335.
[36] U. Schobel, H.-J. Egelhaaf, A. Brecht, D. Oelkrug, G. Gauglitz, Bioconjugate Chem. 10 (1999) 1107–1114.
[37] U. Schobel, H.-J. Egelhaaf, D. Fröhlich, A. Brecht, D. Oelkrug, G. Gauglitz, J. Fluoresc. 10 (2000) 147–154.
[38] B. Ballou, G.W. Fisher, A.S. Waggoner, D.L. Farkas, J.M. Reiland, R. Jaffe, R.B. Mujumdar, S.R. Mujumdar, T.R. Hakala, Cancer Immunol. Immunother. 41 (1995) 257–263.
[39] H.J. Gruber, C.D. Hahn, G. Kada, C.K. Riener, G.S. Harms, W. Ahrer, T.G. Dax, H.-G. Knaus, Bioconjugate Chem. 11 (2000) 696–704.
[40] M.A. Kessler, O.S. Wolfbeis, Anal. Biochem. 200 (1992) 254–259.
[41] M.D. Antoine, S. Devanathan, G. Patonay, Spectrochim. Acta 47A (1991) 501–508.
[42] P. Czerney, F. Lehmann, M. Wenzel, V. Buschmann, A. Dietrich, G.J. Mohr, Biol. Chem. 382 (2001) 495–498.
[43] A. Mishra, R.K. Behera, P.K. Behera, B.K. Mishra, G.B. Behera, Chem. Rev. 100 (2001) 1973–2011.
[44] W. Rettig, K. Rurack, M. Sczepan, From cyanines to styryl bases – photophysical properties, photochemical mechanism, and cation sensing abilities of charged and neutral polymethinic dyes, in: B. Valeur, J.C. Brochon (Eds.), Methods and Applications of Fluorescence Spectroscopy, Springer Verlag, Berlin, PA, 2000, pp. 125–227.
[45] R. Philip, A. Penzkofer, W. Bäumler, R.M. Szeimies, C. Abels, J. Photochem. Photobiol., A 96 (1996) 137–148.
[46] V. Buschmann, K.D. Weston, M. Sauer, Bioconjugate Chem. 14 (2003) 195–204.
[47] G. Colmenarejo, A. Alvarez-Pedraglio, J.L. Lanvadera, J. Med. Chem. 44 (2001) 4370–4378.
[48] K. Licha, B. Riefke, V. Ntziachrisatos, A. Becker, B. Chance, W. Semmler, Photochem. Photobiol. 72 (2000) 392–398.
[49] W.J. Siebrand, Chem. Phys. 44 (1996) 4055–4057.
[50] U. Resch-Genger, Y.Q. Li, J.L. Bricks, V. Kharlanov, W. Rettig, J. Phys. Chem. A 110 (2006) 10956–10971.
[51] Y. Lin, R. Weissleder, C.H. Tung, Bioconjugate Chem. 13 (2002) 605–610.
[52] L.A. Ernst, R.K. Gupta, R.B. Mujumdar, Cytometry 10 (1989) 3–10.
[53] O. Mader, K. Reiner, H.J. Egelhaaf, R. Fischer, R. Brock, Bioconjugate Chem. 15 (2004) 70–78.
[54] Z. Tong, G. Singh, A.J. Rainbow, Photochem. Photobiol. 74 (2001) 707–711.
[55] B. Riefke, K. Licha, W. Semmler, Radiologe 37 (1997) 749–755.
[56] I. Cascorbi, M. Foret, Environ. Saf. 21 (1991) 38–46.
[57] H. Enaida, T. Sakamoto, T. Hisatomi, Y. Goto, T. Ishibashi, Graefes Arch. Clin. Exp. Ophthalmol. 240 (2002) 209–213.
[58] R.M. Sharkey, D.M. Goldenberg, H. Goldenberg, R.E. Lee, C. Ballance, D. Pawlyk, D. Varga, H.J. Hansen, Cancer Res. 50 (1990) 2823–2831.
[59] S.R. Mujumdar, R.B. Mujumdar, C.M. Grant, A.S. Waggoner, Bioconjugate Chem. 7 (1996) 356–362.
[60] U. Resch-Genger, D. Pfeifer, C. Monte, W. Pilz, A. Hoffmann, M. Spieles, K. Rurack, J. Hollandt, D. Taubert, B. Schönenberger, P. Nording, J. Fluoresc. 15 (2005) 315–336.
[61] J.R. Lakowicz, Principles of Fluorescence Spectroscopy, Springer Science + Business Media, New York, PA, third ed., 2006.
[62] R.F. Chen, J. Res. Nat. Bur. Stand. 6 (1972) 593–606.
[63] This formula is valid only for similar excitation wavelengths used for both sample and standard.
[64] S.E. Braslavsky, Glossary of terms used in photochemistry, third ed. (IUPAC Recommendations 2006), Pure Appl. Chem. 79 (2007) 293–465.
[65] K. Rurack, J.L. Bricks, B. Schulz, M. Maus, G. Reck, U. Resch-Genger, J. Phys. Chem. A 104 (2000) 6171–6188.
[66] U. Resch-Genger, K. Hoffmann, W. Nietfeld, A. Engel, J. Neukammer, R. Nitschke, B. Ebert, R. Macdonald, J. Fluoresc. 15 (2005) 337–362.